Available online at www.sciencedirect.com
ScienceDirect
Scripta Materialia 62 (2010) 55–58
Scripta MATERIALIA
www.elsevier.com/locate/scriptamat

# A novel training-free cast Fe–18Mn–5.5Si–9.5Cr–4Ni shape memory alloy with lathy delta ferrite

Y.H. Wen,* H.B. Peng, P.P. Sun, G. Liu and N. Li

*College of Manufacturing Science and Engineering, Sichuan University, Chengdu 610065, People's Republic of China*

Received 8 September 2009; accepted 6 October 2009
Available online 9 October 2009

The microstructures and shape recovery of a cast Fe–18Mn–5.5Si–9.5Cr–4Ni alloy were investigated. We attained lathy ferrite in this cast alloy and a 94% recovery of 3.6% deformation only through annealing this alloy at 973 K. The subdivision of grains by lathy ferrite and its resulting formation of stress-induced martensite bands in a domain-specific manner accounted for the high shape recovery. This work provides a novel idea of developing training-free Fe–Mn–Si shape memory alloy with a high shape recovery.


*Keywords:* Shape memory alloys; Casting; Martensitic phase transformation; Delta ferrite; Domain-specific manners

Low-cost Fe–Mn–Si shape memory alloys (SMAs) have drawn considerable attention over the past 30 years [1–22] as possible alternatives to the expensive Ti–Ni SMAs. Disappointingly, except for some special cases, such as single crystals or thin foil specimens [2,14], the recovery strain (RS) of ordinary polycrystalline Fe–Mn–Si alloys is only 2–3% [1–22], which is far lower than that of Ti–Ni alloys (i.e. 6–8%) [1]. To enhance the RS of Fe–Mn–Si alloys, factors affecting the shape memory effect (SME), such as the alloying elements [5,6], pre-strain level [6,7], deformation temperature [5–7] and thermomechanical treatment, which is referred to as "training" [5,7,9,11,15], have been investigated. The most effective method for improving the SME is training, i.e. the repeated deformation at room temperature (RT) and subsequent annealing at around 923 K. After 3–4 cycles, the RS of ordinary polycrystalline Fe–Mn–Si alloys improves to 4–5% [5,7,9,11]. Not only does training markedly increase the production cost, however; it is also very difficult to perform for alloy components with complicated shapes. Accordingly, current research mainly focuses on developing training-free Fe–Mn–Si SMAs [13–22].

Kajiwara succeeded in improving the RS of an Fe–28Mn–6Si–5Cr–0.5NbC alloy to around 3.8% by producing fine NbC precipitates through an aging process [15]. However, this process only improved the RS of a stainless Fe–15Mn–5Si–9Cr–5Ni–0.5NbC alloy to 3%. Recently, through pre-rolling at 870 K and subsequent aging, they further improved the RS of the Fe–28Mn–6Si–5Cr–0.5NbC and Fe–15Mn–5Si–9Cr–5Ni–0.5NbC alloys to 4.3% and 3.5%, respectively [16]. Unfortunately, the pre-rolling and subsequent aging procedure is essentially a training step [20].

More recently, we proposed that if an austenite grain was first subdivided into smaller domain-specific by crystal defects or phases, then these defects or phases would prevent stress-induced ε martensite (SIEM) bands that belong to different smaller domains from intersecting with each other [21]. Accordingly, SIEM bands would be expected to form in a domain-specific manner (DM). That is to say, in one domain only one group or one dominant group of ε martensite bands is induced. As a result of the formation of SIEM bands in a DM, the collisions between martensite bands and their resultant α′ martensite, which reduced the shape recovery in the Fe–Mn–Si alloys [3,7,8], decreased [21]. Following this proposal, in an Fe–14Mn–5Si–8Cr–4Ni–0.16C alloy, we succeeded in subdividing a grain into smaller domains by lots of aligned $Cr_{23}C_6$ carbides produced by pre-deformation at RT and subsequent aging. During deformation, we made SIEM bands form in a DM, and a RS as high as 4% was attained [21]. The above procedure, however, is still a training step.

Inspired by the result that the subdivision of grains significantly improved the RS by producing a lot of aligned $Cr_{23}C_6$ phases, we thought that if the phases subdividing the grains could be directly introduced during the course of preparing the alloys, and not via

* Corresponding author. E-mail: wenyh-mse@126.com

1359-6462/$ - see front matter © 2009 Acta Materialia Inc. Published by Elsevier Ltd. All rights reserved.
doi:10.1016/j.scriptamat.2009.10.004

a special training step, then it would be possible to develop training-free Fe–Mn–Si SMAs. It is well known that austenitic stainless steels solidify primarily as delta ferrite (δ) when the ratio between the chromium equivalent $Cr_{eq}$ and the nickel equivalent $Ni_{eq}$ is greater than 1.5, and the RT microstructures contain residual vermicular and/or lathy ferrite, depending on the $Cr_{eq}/Ni_{eq}$ value [23–25]. In terms of the morphology of lathy ferrite inside grains, they could also subdivide the grain into smaller domains. Thus, they would also be expected to make SIEM bands form in a DM. Note that almost all studies of Fe–Mn–Si alloys focus on austenitized specimens; few studies focus on as-cast specimens because of the conventional opinion that a good SME can be attained only in Fe–Mn–Si alloys with single-phase austenite [26,27].

To examine this possibility, we designed an Fe–18Mn–5.5Si–9.5Cr–4Ni alloy (in mass%) with a $Cr_{eq}/Ni_{eq}$ value of 1.85, as calculated according to Hammar's equivalents [28]. The experimental alloy was melted and cast into an approximately 6 kg Y-block mold containing sodium silicate sand under an argon atmosphere in an induction - furnace. Specimens with dimensions of 150 mm × 2.0 mm × 1.5 mm were obtained by cutting the Y-block using a Mo filament cutter. Some of specimens were annealed at different temperatures for 30 min, followed by a water quenching.

The shape recovery ratio was examined using bending techniques [20]. An optical color etching method was used to reveal the different phases. The color etching solution comprised 1.2% $K_2S_2O_5$ and 0.5% $NH_4HF_2$ in distilled water. The austenite appears brown; the ε martensite appears white, except that thin plates appear as dark lines; the δ ferrite appears blue; and the σ phase also appears white [12]. The substructures of the specimens were studied using a Tecnai F20 transmission electron microscope. The percentage of ferrite by volume in the specimens was determined with a FERITSCOPE® MP30. The phase transformation temperatures were determined by the resistivity–temperature curve.

Figure 1a shows the optical microstructure of an as-cast Fe–18Mn–5.5Si–9.5Cr–4Ni alloy. As expected, we attained lathy ferrite in addition to some residual vermicular ferrite at RT (black phases). The color optical image at higher magnification (Fig. 1b) showed that some σ phase (white) precipitated inside ferrite (blue). The selected area electron diffraction analyses (Fig. 1c–f) further confirmed this result.

Figure 2 shows the effect of annealing temperature on the shape recovery ratio of the as-cast Fe–18Mn–5.5Si–9.5Cr–4Ni alloy after 3.6% bending deformation. Note that the shape recovery ratio of the as-cast alloy can reach 83% without any special treatment. The shape recovery ratio further increased to 94% after annealing at 973 K for 30 min. Above 973 K, it gradually decreased with increasing temperature up to 1173 K, then rapidly decreased. For conventional polycrystalline Fe–Mn–Si SMAs, such a high shape recovery can only be attained after several cycles of training, while for this novel cast alloy with lathy ferrite, it can only be attained through annealing.

Figure 3 shows the 6% tensile deformation microstructures of an as-cast Fe–18Mn–5.5Si–9.5Cr–4Ni alloy and the cast alloy annealed at different temperatures. For the as-cast Fe–18Mn–5.5Si–9.5Cr–4Ni alloy, the SIEM bands formed in a DM (white parallel bands), as expected. In the I domain in Figure 3, only one group of martensite bands was induced; in II and III domains only one dominant group of martensite bands was induced. In addition, we found that SIEM bands could still form in a DM in specimens annealed at under 1173 K. In specimens annealed at 1273–1423 K, two dominant groups of SIM bands were induced, and collisions between martensite bands occurred more frequently. Note that, as compared to the as-cast specimen, the most SIEM was induced in the specimen annealed at 973 K, less SIEM was induced in specimens annealed at 1173–1273 K and the least SIEM was induced in the specimen annealed at 1423 K.

Figure 4 shows the effects of annealing temperature on the $M_s$ temperature and the volume percentage of

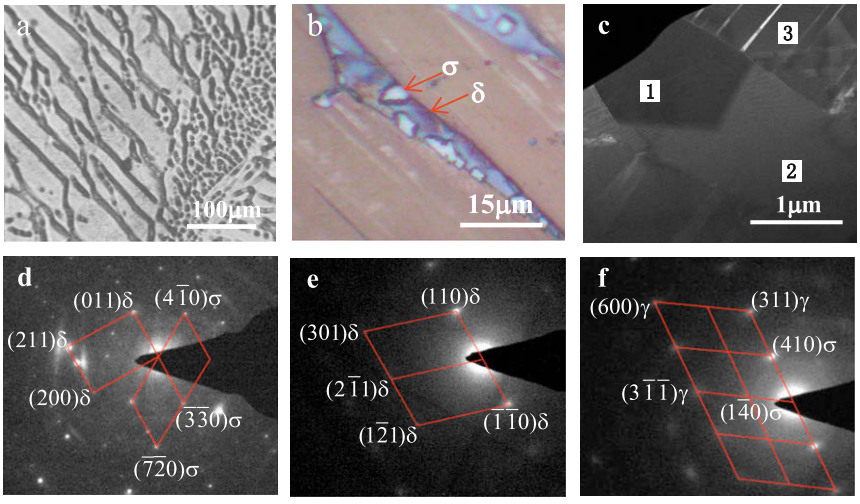


**Figure 1.** Microstructures of the as-cast Fe–18Mn–5.5Si–9.5Cr–4Ni alloy. (a) Optical image; (b) color optical image; (c) transmission electron microscopy bright-field image; (d) selected area diffraction pattern corresponding to area 1 shown in (c); (e) selected area diffraction pattern corresponding to area 2 shown in (c); (f) selected area diffraction pattern corresponding to area 3 shown in (c).

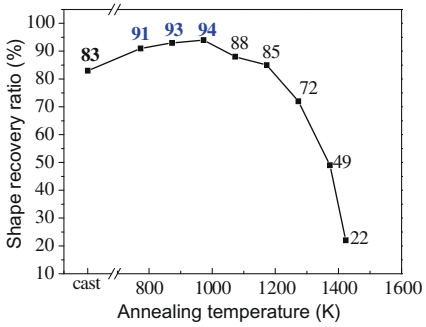


**Figure 2.** Effect of annealing temperatures on the shape recovery ratio of the as-cast Fe–18Mn–5.5Si–9.5Cr–4Ni alloy after 3.6% bending deformation.

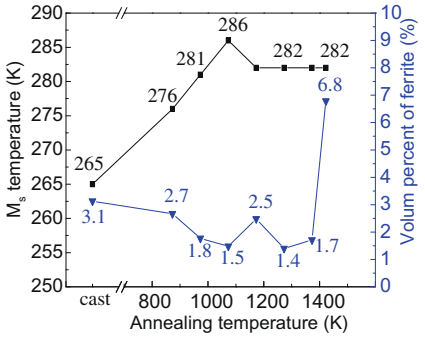


**Figure 4.** Effects of annealing temperature on the $M_s$ temperature and the volume percentage of ferrite in the as-cast Fe–18Mn–5.5Si–9.5Cr–4Ni alloy.

ferrite (VPF). The $M_s$ temperature increased as the temperature increased up to 1073 K, then decreased slightly after annealing at 1173 K; above this temperature it remained almost constant. In contrast, the VPF decreased as the temperature increased up to 1073 K, then increased after annealing at 1173 K. After annealing at 1273 K, the VPF again decreased. After annealing at 1423 K, the VPF increased significantly.

The studies showed that a good SME could be obtained when the deformation occurred around the $M_s$ temperature [5–7,10]. In contrast, the shape recovery ratio of the experimental alloy annealed at 1423 K was far lower than that annealed at 973 K, although its $M_s$ temperature was closer to the deformation temperature, i.e. a RT of 293 K. Obviously, the change of the $M_s$ temperature cannot account for the dramatic change in the shape recovery ratio after annealing. Note that the most SIEM was induced in the specimen annealed at 973 K, while the least was induced in the onr annealed at 1423 K. Therefore, the amount of SIEM accounted for the dramatic change in the shape recovery ratio after annealing.

As mentioned above, in specimens annealed at 1273–1423 K, two dominant groups of SIEM bands were induced and collisions occurred more frequently. The collisions prevented further SIEM transformation and thus decreased the amount of SIEM. To allow the deformation to continue, permanent slip would inevitably be introduced. Obviously, for a given amount of deformation, the smaller the amount of SIEM, the greater the amount of permanent slip. This explains why the shape recovery ratio of the experimental alloy annealed at 1423 K was far lower than that of the alloy annealed at 973 K, although its $M_s$ temperature was closer to the deformation temperature. These results again revealed that it was the collisions between martensite bands that reduced the shape recovery in Fe–Mn–Si alloys [3,7,8]. Furthermore, the formation of SIEM bands can reduce these collisions and thus improve the SME of Fe–Mn–Si alloys remarkably.

In ternary Fe–Cr–Ni and Fe–Cr–Mn alloys, the σ phase appears only when the Cr content is above approximately 15%, which is far higher than that of our experimental alloy. In addition, in Cr–Ni austenitic stainless steels, the σ phase precipitates only after aging for 10 h at above 873 K. However, the addition of Si can shift the σ phase region to that of low Cr content and accelerate the precipitation of the σ phase. When the Si content reaches 2.5%, the σ phase region expands to that of 10% Cr [29]. This explains why some σ phase had already precipitated inside the ferrite in the as-cast Fe–18Mn–5.5Si–9.5Cr–4Ni alloy. With increasing

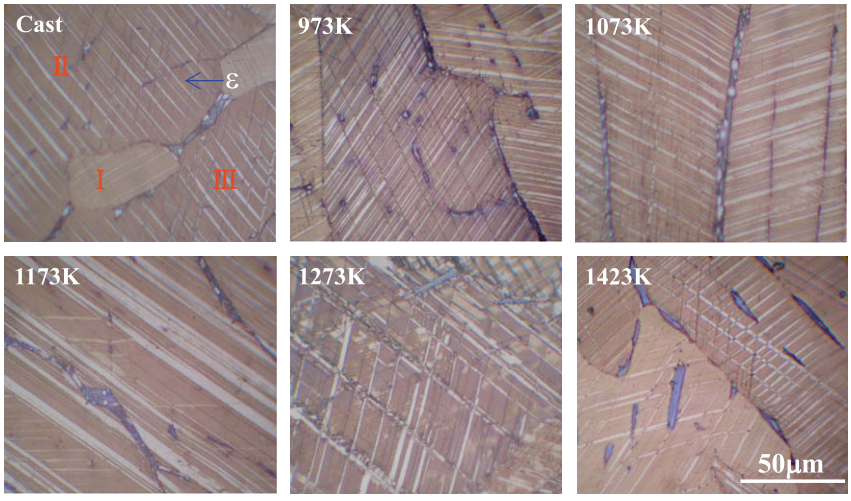


**Figure 3.** Six percentage of tensile deformation microstructures of an as-cast Fe–18Mn–5.5Si–9.5Cr–4Ni alloy and the cast alloy annealed at different temperatures.

annealing temperature, more and more σ phase precipitated. Because the σ phase, like austenite, is a nonmagnetic phase, the precipitation of the σ phase inside ferrite decreased the volume percentage of magnetic phase ferrite. Accordingly, the VPF decreased with increasing annealing temperature up to 1073 K. Over 1073 K, the σ phase began to redissolve into the ferrite and thus the VPF again increased after annealing at 1173 K. Single-phase austenite is thermodynamically in equilibrium at approximately 1273 K, thus ferrite will redissolve in austenite after annealing at 1273 K [23]. Therefore, the VPF again decreased after annealing at 1273 K. When the annealing temperature reached 1423 K, two-phase austenite and ferrite reach thermodynamic equilibrium [23]. As a result, in addition to the precipitation of some ferrite, some of the existing ferrite redissolves into austenite and some small blocks of ferrite coalesce, leading to the remarkable increase of VPF and the morphology of ferrite evolves from lathy to island (Fig. 3). These results indicated that ferrite with lathy morphology could remarkably improve the SME of Fe–Mn–Si alloys, while ferrite with an island morphology could not. The reason may be that the ferrite with island morphology cannot subdivide grains into smaller domains very well and make SIM bands form in a DM. As a result, the collisions between SIEM bands cannot remarkably reduced.

In conclusion, we attained a high shape recovery in a cast Fe–18Mn–5.5Si–9.5Cr–4Ni alloy with lathy delta ferrite only through annealing, not through training. This result again confirmed that the formation of SIEM bands in a domain-specific manners could remarkably improve the shape recovery of Fe–Mn–Si alloys. Our result is of great importance. Above all, it presents a novel idea of developing training-free Fe–Mn–Si SMAs with high RS. Secondly, it holds great promise for further improving shape recovery of cast Fe–Mn–Si SMAs through modifying and optimizing alloy compositions with solidification parameters and the heat treatment technique. Finally, casting is a versatile and cost-efficient manufacturing technique, and thus our finding will promote the use of Fe–Mn–Si SMAs in engineering areas.

The work was supported by the National Natural Science Foundation of China (Nos. 50501015 and 50871072) and the Program for New Century Excellent Talents in University (No. NCET-06-0793).

[1] K. Otsuka, C.M. Wayman, Shape Memory Materials, Cambridge University Press, New York, 1998.
[2] A. Sato, E. Chishima, K. Soma, T. Mori, Acta Metall. Mater. 30 (1982) 1177.
[3] A. Sato, E. Chishima, Y. Yamaji, T. Mori, Acta Metall. Mater. 32 (1984) 539.
[4] A. Sato, Y. Yamaji, T. Mori, Acta Metall. Mater. 34 (1986) 287.
[5] H. Otsuka, H. Yamada, T. Maruyama, H. Tanahashi, S. Matsuda, M. Murakami, ISIJ Inter 30 (1990) 674.
[6] J.H. Yang, H. Chen, C.M. Wayman, Metall. Mater. Trans. A 23 (1992) 1431.
[7] H. Inagaki, Z. Metall. 83 (1992) 90.
[8] H. Inagaki, Z. Metall. 83 (1992) 97.
[9] X.X. Wang, L.C. Zhao, Scripta Mater. Metall. 26 (1992) 1451.
[10] Q. Gu, J. Van Humbeeck, L. Delaey, J. Phys. IV 4 (1994) 135.
[11] D.F. Wang, Y.R. Chen, F.Y. Gong, D.Z. Liu, W.X. Liu, J. Phys. IV 5 (1995) 527.
[12] N. Bergeon, G. Guenin, C. Esnouf, Mater. Sci. Eng. A 242 (1998) 77.
[13] S. Kajiwara, Mater. Sci. Eng. A 273–275 (1999) 67.
[14] A. Sato, T. Masuya, M. Morishita, S. Kumai, A. Inoue, Mater. Sci. Forum 327–328 (2000) 223.
[15] S. Kajiwara, D. Liu, T. Kikuchi, N. Shinya, Scripta Mater. 44 (2001) 2809.
[16] A. Baruj, T. Kikuchi, S. Kajiwara, N. Shinya, Mater. Sci. Eng. A 378 (2004) 333.
[17] Y.H. Wen, M. Yan, N. Li, Scripta Mater. 50 (2004) 441.
[18] Y.H. Wen, M. Yan, N. Li, Scripta Mater. 50 (2004) 835.
[19] Z.Z. Dong, S. Kajiwara, T. Kikuchi, T. Sawaguchi, Acta Mater. 53 (2005) 4009.
[20] N. Stanford, D.P. Dunne, J. Mater. Sci. 41 (2006) 4883.
[21] Y.H. Wen, W. Zhang, N. Li, H.B. Peng, L.R. Xiong, Acta Mater. 55 (2007) 6526.
[22] N. Stanford, D.P. Dunne, H. Li, Scripta Mater. 58 (2008) 583.
[23] J.C. Lippold, D.J. Kotecki, Welding Metallurgy and Weldability of Stainless Steel, John Wiley & Sons Inc., Hoboken, NJ, 2005.
[24] N. Suutala, T. Takalo, T. Moisio, Metall. Mater. Trans. A 10 (1979) 512.
[25] G.L. Leone, H.W. Kerr, Welding J. 61 (1982) 13.
[26] H. Kubo, H. Otsuka, S. Farjamic, T. Maruyama, Scripta Mater. 52 (2006) 1059.
[27] J.C. Li, M. Zhao, Q.J. Jiang, Mater. Eng. Perform. 11 (2002) 313.
[28] N. Suutala, Metall. Mater. Trans. A 13 (1982) 2121.
[29] E. Folkhard, Welding Metallurgy of Stainless Steel, Springer-Verlag, Wein, 1988.